



Technological University Dublin  
ARROW@TU Dublin

---

Articles

Centre for Elastomer Research

---

2017

## Application of Phase Shifting Electronic Speckle Pattern Interferometry in Studies of Photoinduced Shrinkage of Photopolymer Layers

Mohesh Moothanchery

*Nanyang Technological University, Singapore, moheshm@gmail.com*

Viswanath Bavigadda

*European Gravitational Observatory, Italy, viswanath.bavigadda@student.dit.ie*

Manojit Pramanik

*Nanyang Technological University, Singapore*

Vincent Toal

*Technological University Dublin, vincent.toal@tudublin.ie*

Follow this and additional works at: <https://arrow.tudublin.ie/cerart>

Isabela Naydenova

*Technological University Dublin, izabela.naydenova@tudublin.ie*

Part of the [Optics Commons](#), and the [Polymer and Organic Materials Commons](#)

---

### Recommended Citation

Moothanchery, M. (2017). Application of Phase Shifting Electronic Speckle Pattern Interferometry in Studies of Photoinduced Shrinkage of Photopolymer Layers. *Optical Express*, vol. 25, no. 9, pp. 9647-9653. doi: 10.1364/OE.25.009647.

This Article is brought to you for free and open access by the Centre for Elastomer Research at ARROW@TU Dublin. It has been accepted for inclusion in Articles by an authorized administrator of ARROW@TU Dublin. For more information, please contact [yvonne.desmond@tudublin.ie](mailto:yvonne.desmond@tudublin.ie), [arrow.admin@tudublin.ie](mailto:arrow.admin@tudublin.ie), [brian.widdis@tudublin.ie](mailto:brian.widdis@tudublin.ie).



This work is licensed under a [Creative Commons Attribution-Noncommercial-Share Alike 3.0 License](#)



# Application of Phase Shifting Electronic Speckle Pattern Interferometry in Studies of Photoinduced Shrinkage of Photopolymer layers

MOHESH MOOTHANCHERY,<sup>1,\*</sup> VISWANATH BAVIGADDA,<sup>2,3</sup>

MANOJIT PRAMANIK,<sup>1</sup> VINCENT TOAL,<sup>3</sup> AND IZABELA NAYDENOVA,<sup>3</sup>

<sup>1</sup>*School of Chemical and Biomedical Engineering, Nanyang Technological University, Singapore*

<sup>2</sup>*European Gravitational Observatory, Cascina PI, Italy*

<sup>3</sup>*Centre for Industrial and Engineering Optics, School of Physics, Dublin Institute of Technology, Ireland*

<sup>4</sup>*izabela.naydenova@dit.ie*

*\*mmohesh@ntu.edu.sg*

**Abstract:** Photoinduced shrinkage occurring in photopolymer layers during holographic recording was determined by Phase Shifting Electronic Speckle Pattern Interferometry. Phase maps were calculated from the changes in intensity at each pixel due to the phase differences introduced between object and reference beams. Shrinkage was then obtained from the changes in phase as recording proceeded. The technique allows for whole field measurement of the dimensional changes in photopolymers during holographic recording.

© 2017 Optical Society of America

**OCIS codes:** (090.0090) Holography; (120.6165) Speckle Interferometry, Metrology; (160.5470) Polymers; (090.7330) Volume gratings.

---

## References and links

1. S. Martin, C. A. Feely, and V. Toal, "Holographic recording characteristics of an acrylamide based photopolymer," *Appl. Opt.* **36**, 5757-5768 (1997).
  2. M. Moothanchery, I. Naydenova, V. Bavigadda, and V. Toal, "Shrinkage during holographic recording in photopolymer films determined by holographic interferometry," *Applied Optics*. **52**, 8519-8527 (2013).
  3. M. Moothanchery, I. Naydenova, and V. Toal, "Study of the shrinkage caused by holographic grating formation in acrylamide based photopolymer film," *Optics Express*. **19**, 13395-13404 (2011).
  4. M. Moothanchery, I. Naydenova, and V. Toal, "Studies of shrinkage as a result of holographic recording in acrylamide based photopolymer film," *Appl. Physics, A*. **104**, 899-902 (2011).
  5. C. Neipp, A. Beléndez, S. Gallego, M. Ortuño, I. Pascual, and J. T. Sheridan, "Angular responses of the first and second diffracted orders in transmission diffraction grating recorded on photopolymer material," *Optics Express*. **11**, 1835- 1843 (2003).
  6. H. Sherif, I. Naydenova, S. Martin, C. McGinn and V. Toal, "Characterization of an acrylamide based photopolymer for data storage utilizing holographic angular multiplexing," *J. Opt. A: Pure Appl. Opt.* **7**, 255–260 (2005).
  7. Mingju Huang, Huawen Yao, Zhongyu Chen, Lisong Hou, and Fuxi Gan, The changes of holographic characteristics of photopolymer induced by temperature, *Chinese Optics Letters*. **1**, 41-43 (2003).
  8. O. J. Lokberg, "Advances and Applications of Electronic Speckle Pattern Interferometry (ESPI)," *Proc. Soc.Photo-Opt. Instrum. Eng.* 215, 92 (1980).
  9. O. J. Lokberg and K. Hogmoen, "Use of modulated reference wave in electronic speckle pattern interferometry," *J. Phys. E: Sci. Instr.* **9**, 847-851 (1976).
  10. M. Moothanchery, V. Bavigadda, P. Kumar Upputuri, M. Pramanik, V. Toal, I. Naydenova, "Quantitative measurement of displacement in photopolymer layers during holographic recording using phase shifting electronic speckle pattern interferometry," *Proc. SPIE*. **9718**, 9718C-1 (2016).
  11. M. Moothanchery, S. Mintova, I. Naydenova and V. Toal, "Si-MFI zeolite nanoparticle doped photopolymer with reduced shrinkage," *Optics Express*. **19**, 25786-25791(2011).
  12. J. Schwider, R. Burow, K. E. Elssner, J. Grzanna, R. Spolaczyk and K. Merkel, "Digital wavefront measuring interferometry--some systematic error sources," *Appl. Opt.* **22**, 3421-3432 (1983).
  13. W.H.Stevenson, "Optical frequency shifting by means of rotating a diffraction grating," *Appl. Opt.* **9**, 649-652 (1970).
  14. M. A. Herraes, D. R. Burton, M. J. Lalor, M. A. Gdeisat "Fast two-dimensional phase unwrapping algorithm based on sorting by reliability following a noncontinuous path," *Appl. Opt.* **41**, 7437-744 (2002).
  15. K.Creath, "Phase shifting speckle interferometry," *Appl. Opt.* **24**, 3053-3058 (1985)
-

16. E.Hata and Y.Tomita, "Stoichiometric thiol-to-ene ratio dependence of refractive index modulation and shrinkage of volume gratings recorded in photopolymerizable nanoparticle polymer composites based on step-growth polymerization," *Opt. Mater. Express* **1**, 1113–1120 (2011).
- 

## 1. Introduction

Change in angular position of the Bragg diffraction peak due to shrinkage in photopolymers is a significant disadvantage in applications such as holographic data storage and holographic optical elements. The effect of shrinkage will result in Bragg mismatch during reconstruction and the readout beam direction needs to be altered otherwise only a portion of data page can be read out for a particular readout geometry, which leads to large data errors. Compensation is required for the detuning of the Bragg angle and for that reason development of materials with low shrinkage is necessary. In order to achieve this an in-depth understanding of the processes influencing the shrinkage during holographic recording is required. Acrylamide based photopolymers are one of the most studied holographic recording materials. Shrinkage occurring during holographic recording in an acrylamide-based photopolymer [1] has been determined using real time holographic interferometry [2] and by measuring the shift in the angular position of the Bragg peak of a holographically recorded diffraction grating [3-6]. The measurements are typically made of the diffraction efficiency at a single point of the recorded holographic grating. Using this technique it has been established previously that monomer diffusion plays an important role in holographic recording [7] and it occurs simultaneously with the layer shrinkage. Alternatively, electronic speckle pattern interferometry (ESPI) can be used to measure in-plane and out-of-plane components of displacement continuously and independently of each other making it useful for determining whole field surface deformation and shrinkage. Lokberg [8] reported the use of a phase shifting technique in speckle interferometry to measure object displacement. Moving a mirror in the reference beam path by means of piezoelectric transducer is one of the most common techniques [9,10] for phase shifting. Phase shifting electronic speckle pattern interferometry was the technique of choice in this study because of its whole field and near real-time capability.

## 2. Experimental Procedures

The photopolymer solution was prepared as previously described [11]. Briefly, 0.6 g of acrylamide monomer was added to 9 ml stock solution of polyvinyl alcohol in water (20% wt/wt). Then 0.2 g of N, N-methylene bisacrylamide was added. To this solution 2 ml of triethanolamine and 4 ml of Erythrosine-B dye (0.11% wt. water stock solution) was added. Volumes of 0.3 ml were spread completely on 25 mm × 35 mm glass plates. The sample thicknesses in the area of recording after drying were approximately  $100 \pm 3 \mu\text{m}$ . Similarly volumes of 0.1 ml and 0.2 ml were spread on circular regions 1 cm and 1.4 cm in diameter respectively on a similar glass plate. The thickness after drying was  $160 \pm 3 \mu\text{m}$ . The ESPI system is as shown in Fig. 1. Shrinkage during holographic recording was measured in a photopolymer film photosensitized with green light sensitive dye - Erythrosin B (ErB). The glass substrate of the photopolymer was coated on its other side with non-reflective paint, to prevent back reflection of light from the glass. A similar glass plate, attached to a piezoelectric transducer (PZT) was used for phase shifting. The speckle interferometer beam paths are shown in red in Fig. 1. The beam produced by a He-Ne laser was split in two. The object beam reflected from the ErB sample and the reference beam partially reflected from the piezoelectrically driven glass plate were allowed to interfere on a CMOS camera faceplate (pixel size:  $6 \mu\text{m} \times 6 \mu\text{m}$ ). The angular separation between the object and the reference beams was  $90^\circ$ . The field of view of the camera was 25 mm in width. The photopolymer film was exposed to an interference pattern produced by laser light of 532 nm wavelength at a spatial frequency of 1000 lines/mm with an angular separation between the two beams  $30.85^\circ$ . The paths of the interfering beams are shown in green in Fig. 1(a). The intensity profile of the 532 nm laser is shown in Fig. 1(b).

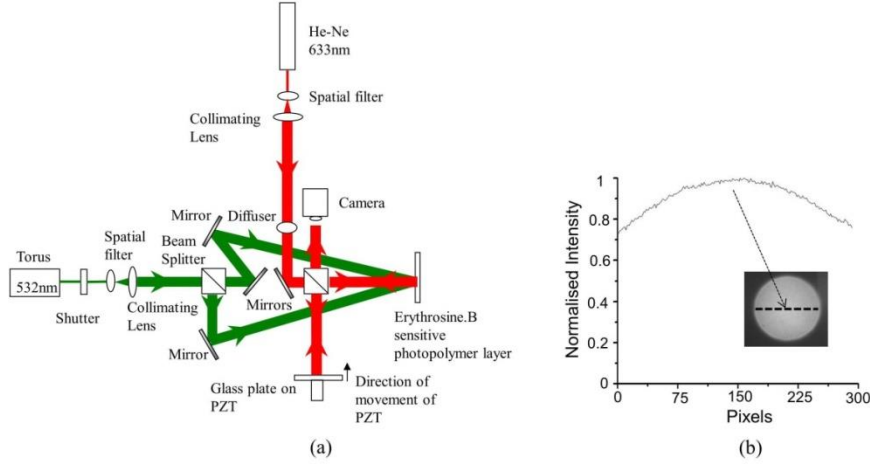


Fig. 1. (a) ESPI system Light paths in green represent beams used to record a holographic diffraction grating in the photopolymer layer. Light paths in red are those of the speckle interferometer. (b) Intensity profile of recording beam.

The PZT was controlled to produce phase shifts of  $90^\circ$  at 632.8 nm. Five phase shifted frames were stored for the unexposed layer. After exposure to the 532 nm interference pattern for predetermined amounts of time 5 new phase shifted frames were captured and stored. Phase shifted frames were captured and stored for different exposure time intervals. The five frame algorithm was used [12] to obtain phase maps, the phase  $\phi$  being given by

$$\phi = \tan^{-1} \left[ \frac{2(I_4 - I_2)}{I_1 - 2I_3 + I_5} \right] \quad (1)$$

Where  $I_1, I_2, I_3, I_4, I_5$  are the intensities of the interferograms with phase steps of  $-\pi, -\frac{\pi}{2}, 0, \frac{\pi}{2}, \pi$ . The phase value at each pixel lies in  $-\pi, +\pi$  range. Gray level zero corresponds to phase value of  $-\pi$  and saturated white pixels correspond to phase value of  $+\pi$

The phase map calculated from these 5 phase shifted frames contains  $2\pi$  phase discontinuities. Phase unwrapping is the process of removing these  $2\pi$  phase steps [13]. One method of phase unwrapping is by calculating the phase difference between adjacent pixels by scanning along each row or column. Whenever phase jumps are detected, depending on the sign of the jump,  $2\pi$  is either subtracted or added from the pixel's phase value. The wrapped phase maps obtained before and during holographic exposure were unwrapped using the 2D-SRNCP unwrapping algorithm [14] which belongs to the class of quality guided path algorithms. To prevent error propagation, this algorithm unwraps the pixels with highest reliability values first and those with lowest reliability value last. Reliability in this algorithm is determined by the second differences (meaning difference of phase gradients) between the pixel and its neighbours. In this way inconsistencies in the phase map can be reduced. The algorithm follows non-continuous paths for unwrapping. The phase maps still contain some errors which cannot be detected, but the algorithm is very robust in practice compared to continuous path unwrapping algorithms.

An unwrapped phase map before exposure is shown in Fig. 2 (a). The unwrapped phase map after 84 sec exposure is shown in Fig. 2(b). The unwrapped phase maps corresponding to the sample surface profile before and after exposure were subtracted from one another to obtain Fig. 2(c) from which a 3D displacement map representing the shrinkage was calculated using Eq. 2 [15].

$$d = \left( \frac{\lambda}{4\pi} \right) \phi \quad (2)$$

where,  $\Delta d$  - shrinkage in photopolymer layer;  $\lambda$  - wavelength of laser;  $\phi$  - unwrapped phase

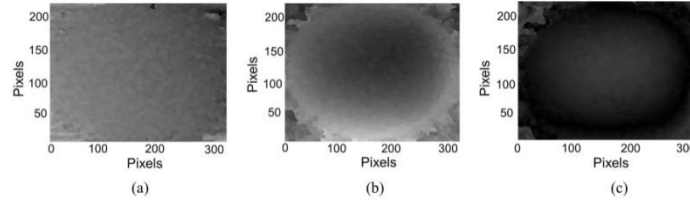


Fig. 2. Unwrapped phase maps (a) before exposure (b) after 84 sec exposure (c) result of subtracting a from b.

Since the shrinkage in lateral direction is small the developed system would be an ideal tool to determine out-of-plane shrinkage profile in photopolymer layers during holographic recording. Shrinkage in photopolymer materials is attributed to formation of long polymer chains with morphologies differing from that of monomer molecules. Photopolymerisation thus leads to increased density, accompanied by shrinkage.

In order to determine the shrinkage profile of photopolymer during holographic exposure a 100  $\mu\text{m}$  photopolymer layer was exposed to 5  $\text{mW}/\text{cm}^2$  laser intensity and phase shifted frames were captured at 21 sec, 42 sec, 84 sec and 168 sec of holographic exposure. The circular region of exposure was 2.3 cm in diameter. Figs. 3(a) – 3(d) shows the two dimensional profile of absolute shrinkage at different times of exposures. The three dimensional profile of the white dotted area is shown in Figs. 3(e)- 3(h).

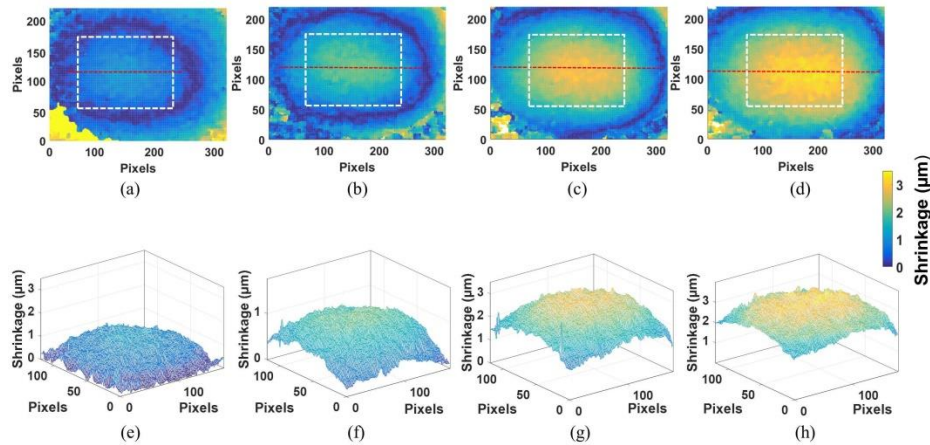


Fig. 3. Two dimensional profile of absolute shrinkage of  $100 \pm 3 \mu\text{m}$  sample at (a) 21 sec (b) 42sec (c) 84sec (d) 168sec of exposure, Three dimensional profile of the white dotted area in the 2D profile is shown from (e)-(h), recording intensity 5  $\text{mW}/\text{cm}^2$

From Fig. 3 we can see that the shrinkage increases almost linearly with exposure time and then reaches saturation after about 100 sec. The line profiles in Fig. 4(a) are cross sections through the centres of the 2D maps (shown in red dotted line). We see from the line profile that the shrinkage is around 0.8  $\mu\text{m}$  after 21 sec of recording. At 42 sec the maximum shrinkage is around 1.8  $\mu\text{m}$ , at 84 sec it is 2.8  $\mu\text{m}$  and at 168 sec it is 3.2  $\mu\text{m}$ . Figure 4(b) shows shrinkage versus time at different pixels across a line through the centre of the map. In the shrinkage profiles 100 pixels corresponds to 7.5 mm. We see that the shrinkage is greater in the centre and is lower towards the edges. We could relate the increased shrinkage at the center to the Gaussian

intensity profile of the recording laser. The data shows how with one single measurement a map of the shrinkage rather than a single point measurement can be carried out.

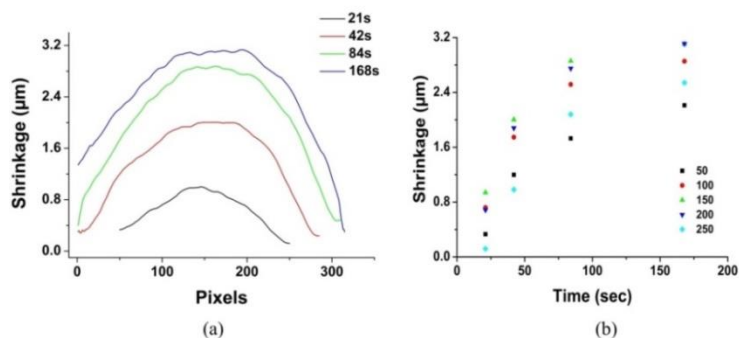


Fig. 4. (a) Absolute shrinkage of 100  $\mu\text{m}$  sample at recording intensity 5  $\text{mW}/\text{cm}^2$  (b) Plot of shrinkage versus exposure times at different pixel number.

We also have studied the effect of recording intensity on a  $160 \pm 3 \mu\text{m}$  sample by keeping the total exposure energy constant using intensities of 1  $\text{mW}/\text{cm}^2$ , 5  $\text{mW}/\text{cm}^2$  and 10  $\text{mW}/\text{cm}^2$ . The exposure time times were 210 sec, 42 sec, and 21 sec respectively. The change in line profile of shrinkage with recording intensity is shown in Fig. 5 which shows that the shrinkage is greater for lower intensities. At lower intensity, the rate at which free radicals are generated is lower leading to a lower rate of termination resulting in longer polymer chains. Long polymer chains are more entangled and the polymerized material is likely to be denser and exhibit greater shrinkage.

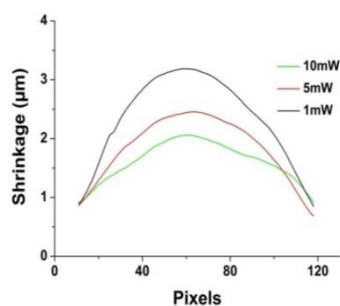


Fig. 5. Absolute shrinkage of 160  $\mu\text{m}$  sample at exposure energy 210  $\text{mJ}/\text{cm}^2$ .

It has been previously demonstrated [16] that shrinkage of photopolymer layers can be decreased by decreasing the length of the created polymer chains. In order to study the effects of monomer diffusion on the displacement profile of photopolymer layers during holographic recording, two sets of experiments were carried out. In the first set the circular exposure region (1 cm in diameter) was smaller in area than the photopolymer layer, allowing for the polymerisation driven monomer diffusion from the unexposed to the exposed area to take place. In the second set of experiments the exposure region is the same as that the photopolymer layer, thus the effect of monomer diffusion is excluded. We have observed a reduction in shrinkage due to diffusion of monomer molecules from the unexposed regions. Samples of thickness  $160 \pm 3 \mu\text{m}$  were exposed for 21 sec, 42 sec and 84 sec respectively with recording intensity 10  $\text{mW}/\text{cm}^2$ . Fig. 6 (a) shows the shrinkage profile of recordings made after 21 sec of exposure. The black line shows the shrinkage profile when the sample area is smaller and the red line shows the profile when the sample area is larger than the exposure area. Similarly Figs. 6(b) and 6(c) show the shrinkage profiles after 42 sec and 84 sec of exposure. We can clearly see

that diffusion plays a crucial role in shrinkage. In the case of holographic recording where the photopolymer layer is smaller in area than the exposure area, the shrinkage is greater at the center as well as at the edges. We can relate this to the fact there is no diffusion of monomer molecules from outside the exposure region. Considering a circular region of diameter 1cm the percentage differences in shrinkage as a result of monomer diffusion were 31%, 60% and 44 % respectively. While in the first 42sec the % shrinkage difference due to monomer diffusion increases almost linearly with time, further increase of exposure time leads to a decrease in shrinkage difference. This could be related to the fact that the diffused monomers were being polymerised as time progresses and also that their diffusion rate has been reduced. More detailed studies would be needed to properly evaluate the role of monomer diffusion on shrinkage dynamics.

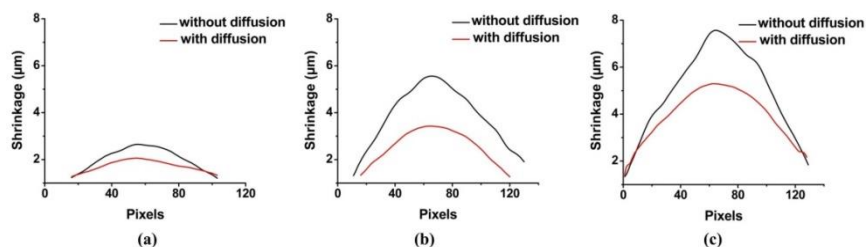


Fig. 6. Effect of diffusion on shrinkage on a 160µm sample (a) 21sec of exposure (b) 42sec of exposure, (c) 84sec of exposure, recording intensity 10mW/cm<sup>2</sup>.

### 3. Conclusions

We have demonstrated measurement of whole-field deformation due to holographic recording in photopolymer, using a phase shifting ESPI system. Phase shifted specklegrams were captured before and after holographic recording for different recording times and intensities. These phase shifted specklegrams were used to obtain unwrapped phase maps before and after exposure. These maps were then subtracted from each other to obtain the shrinkage profile as a phase map and finally the actual full-field shrinkage profiles. It was observed that the shrinkage has its maximum in the center of the illumination spot and increases with the recording time. The dynamics of the shrinkage depends on the intensity of recording, a result that is consistent with previously reported data obtained from Bragg shift measurements in acrylamide based photopolymer holographic gratings. From the results presented here we can confirm that the recording beam intensity profile as well as diffusion from outside the recording area will influence shrinkage. The technique described here will find application in the characterization of photosensitive polymer materials for holographic applications.

### Acknowledgments

This work was supported by DIT Fiosraigh Research Scholarship programme. The authors would like to thank the School of Physics DIT and the Focas Research Institute, DIT, for technical support.

### Funding

The authors would also like to acknowledge the financial support from Tier 2 grant funded by the Ministry of Education in Singapore (ARC2/15: M4020238).